PHASES OF STRONGLY INTERACTING MATTER IN THE BRAHMS EXPERIMENT

P. STASZEL[4]

FOR THE BRAHMS COLLABORATION

I. ARSENE[12], I. G. BEARDEN[7], D. BEAVIS[1], S. BEKELE[11], C. BESLIU[10], B. BUDICK[6], H. BØGGILD[7], C. CHASMAN[1], C. H. CHRISTENSEN[7], P. CHRISTIANSEN[7], R. CLARKE[10], R. DEBBE[1], J. J. GAARDHØJE[7], K. HAGEL[8], H. ITO[11], A. JIPA[10], J. I. JØRDRE[9], F. JUNDT[2], E. B. JOHNSON[11], C. E. JØRGENSEN[7], R. KARABOWICZ[4], N. KATRYŃSKA[4], E. J. KIM[1], T. M. LARSEN[7], J. H. LEE[1], Y. K. LEE[5], S. LINDAL[12], G. LØVHØIDEN[12], Z. MAJKA[4], M. MURRAY[11], J. NATOWITZ[8], B. S. NIELSEN[7], D. OUERDANE[7], R. PŁANETA[4], F. RAMI[2], C. RISTEA[7], O. RISTEA[10], D. RÖHRICH[9], B. H. SAMSET[12], S. J. SANDERS[11], R. A. SHEETZ[1], P. STASZEL[4], T. S. TVETER[12], F. VIDEBÆK[1], R. WADA[8], H. YANG[9], Z. YIN[9], I. S. ZGURA[10]

[1] *Brookhaven National Laboratory, Upton,New York 11973,* [2] *Institut de Recherches Subatomiques and Université Louis Pasteur, Strasbourg, France,* [3] *Institute of Nuclear Physics, Krakow, Poland,* [4] *Jagiellonian University, Krakow, Poland,* [5] *Johns Hopkins University, Baltimore, Maryland 21218,* [6] *New York University, New York, New York 10003,* [7] *Niels Bohr Institute, University of Copenhagen, Denmark,* [8] *Texas A&M University, College Station,Texas 77843,* [9] *University of Bergen, Department of Physics, Bergen,Norway,* [10] *University of Bucharest,Romania,* [11] *University of Kansas, Lawrence, Kansas 66049,* [12] *University of Oslo, Department of Physics, Oslo,Norway* [+] *Deceased*

We review results obtained by the BRAHMS experiment at the Relativistic Heavy Ion Collider (RHIC) for the systems of Au+Au and Cu+Cu colliding at $\sqrt{s_{NN}} = 200$ GeV and at 62.4 GeV, and p+p colliding at $\sqrt{s_{NN}} = 200$ GeV. The observed number of charged particles produced per unit of rapidity in the central rapidity region indicates that a high energy density system is produced at the initial stage of the Au+Au reaction. Analysis of anti-particle to particle ratios as a function of rapidity and collision energy reveal that particle populations at the chemical freeze-out stage for heavy-ion reactions at and above SPS energies are controlled by the baryon chemical potential. We present rapidity dependent p/π ratios within $0 < y < 3$ for Au+Au and Cu+Cu at $\sqrt{s_{NN}} = 200$ GeV. The ratios are enhanced in nucleus-nucleus collisions as compared to p+p collisions. The particle ratios are discussed in terms of their system size and rapidity dependence. We compare R_{AA} for Au+Au at $\sqrt{s_{NN}} = 200$ GeV and at 62.4 GeV, and for Au+Au and Cu+Cu at $\sqrt{s_{NN}} = 62.4$ GeV. R_{AA} is found to increase with decreasing collision energy, decreasing system size, and when going towards more peripheral collisions. However, R_{AA} shows only a very weak dependence on rapidity (for $0 < y < 3.2$), both for pions and protons.

Keywords: RHIC;QGP;Nuclear Modification Factor;high rapidity

1. Introduction

Reactions between heavy nuclei provide a unique opportunity to produce and study nuclear (hadronic) matter far from its ground state, at high densities and temperatures. From the onset of the formulation of the quark model and the first understanding of the nature of the binding and confining potential between quarks about 30 years ago, it has been realized that at very high density and temperature, hadronic matter may undergo a transition to a more primordial form of matter. This proposed state of matter named the quark gluon plasma (QGP) [1], is characterized by a strongly reduced interaction among its constituents, quarks and gluons, such that the partons would exist in a nearly free state [2].

In mid-August 2001 systematic data collecting by the four RHIC experiments, namely BRAHMS [3], PHENIX [4], PHOBOS [5] and STAR [6], began at the energy of $\sqrt{s_{NN}} =$ 200 GeV. The RHIC operations started a new era of studies of ultra-relativistic nucleus-nucleus collisions. BRAHMS (Broad RAnge Hadron Magnetic Spectrometers) [7], consists of set of detectors designed to measure global features of the collision like overall charged particle multiplicity and the flux of spectator neutrons, and of two spectrometer arms that provide the measurement of the full particle four-momentum vector. By rotating the arms within the small (from 2 to 30 degree) and large particle emission angles (from 30 to 90 degree) BRAHMS is able to study the properties of the produced medium as a function of its longitudinal expansion.

2. Overall bulk charakteristics

The multiplicity distribution of emitted particles is a fundamental observable in ultra-relativistic collisions. It is sensitive to all stages of the reaction and can address issues such as the role of hard scatterings between partons and the interaction of these partons in the high-density medium [8,9,10].

For central collisions at $\sqrt{s_{NN}} =$ 200 GeV we observe about 4500 charged particles within the rapidity range covered by the detection system and $\mathrm{dN}_{ch}/\mathrm{d}\eta\ |_{\eta=0} = 625 \pm 56$. The latter value, if scales with the number of participant pairs, exceeds the particle production observed in elementary p+$\bar{\mathrm{p}}$ collisions at the same energy by 40 - 50% [11]. This means that nucleus-nucleus collisions at the considered energies are far from being the simple superposition of elementary nucleon-nucleon collisions.

The measurement of charged particle density $dN_{ch}/d\eta$ can be used to estimate the so-called Bjorken energy density, ε [12]. The results obtained from identified particle abundances and particle spectra measured for central collisions lead to values of ε equal 5 GeV/fm^3 at $\sqrt{s_{NN}}$ = 200 GeV, 4.4 GeV/fm^3 at $\sqrt{s_{NN}}$ = 130 GeV, and 3.7 GeV/fm^3 at $\sqrt{s_{NN}}$ = 62.4 GeV assuming formation time of 1 fm/c [13]. All of these values significantly exceed the predicted energy density $\varepsilon \approx 1$ GeV/fm^3 for the boundary between hadronic and partonic phases of nuclear matter [14].

2.1. *Hadrochemistry with BRAHMS data*

BRAHMS measures anti-particle to particle ratios for pions, N_{π^-}/N_{π^+}, kaons, N_{K^-}/N_{K^+}, and protons, $N_{\bar{\mathrm{p}}}/N_{\mathrm{p}}$, over a large rapidity interval. For Au+Au collision at $\sqrt{s_{NN}}$ = 200 GeV and $\sqrt{s_{NN}}$ = 62.4 GeV N_{π^-}/N_{π^+} stays constant and is equal to 1 over the covered rapidity range (0 < y < 3.2). The N_{K^-}/N_{K^+} and $N_{\bar{\mathrm{p}}}/N_{\mathrm{p}}$ ratios drop significantly with increasing rapidity. For $\sqrt{s_{NN}}$ = 200 GeV the N_{K^-}/N_{K^+} and $N_{\bar{\mathrm{p}}}/N_{\mathrm{p}}$ ratios are equal, respectively to 0.95 and 0.76 at $y \approx 0$, and reach values of 0.6 for N_{K^-}/N_{K^+} and 0.3 for $N_{\bar{\mathrm{p}}}/N_{\mathrm{p}}$ around rapidity 3.

Figure 1 shows the N_{K^-}/N_{K^+} ratio as a function of the corresponding $N_{\bar{\mathrm{p}}}/N_{\mathrm{p}}$ for various rapidities. The presented results were obtained for central collisions at three RHIC collision energies. The AGS and SPS results are plotted for comparison. There is a striking correlation between the RHIC/BRAHMS kaon and proton ratios over 3 units of rapidity. It is worth noting that the BRAHMS forward rapidity data measured at $\sqrt{s_{NN}} =$ 62.4 GeV overlap with the SPS points that were measured at much lower energy but at mid-rapidity. The solid line in Figure 1 shows a fit with a statistical model to the $\sqrt{s_{NN}}$ = 200 GeV results only, assuming that the temperature at the chemical freeze-out is 170 MeV [15,16]. It is seen that the data are very well described by the statistical model over a broad rapidity range with the baryon chemical potential changing from 27 MeV at mid-rapidity to 140 MeV at the most forward rapidities. Using simple statistical models at the quark level with chemical and thermal equilibrium, the ratios can be written

$$\frac{N_{\bar{p}}}{N_p} = e^{-6\mu_{u,d}/T}, \qquad \frac{N_{K^-}}{N_{K^+}} = e^{-2(\mu_{u,d}-\mu_s)/T} \quad (1)$$

where μ and T are the chemical potential and temperature, respectively. Substituting $\mu_s = 0$ into eqs. (1), one gets $N_{K^-}/N_{K^+} = [N_{\bar{\mathrm{p}}}/N_{\mathrm{p}}]^{1/3}$. This relation, represented by the dotted line on Figure 1, does not reproduce the observed correlation. The data are, however, well fitted by the function $N_{K^-}/N_{K^+} = [N_{\bar{\mathrm{p}}}/N_{\mathrm{p}}]^{1/4}$ (dashed line) which can be derived from eqs. (1) assuming $\mu_s = 1/4\mu_{u,d}$.

Recently, STAR and NA49 have measured mid-rapidity ratios $\bar{\Lambda}/\Lambda$, $\bar{\Xi}/\Xi$ and $\bar{\Omega}/\Omega$ versus $N_{\bar{\mathrm{p}}}/N_{\mathrm{p}}$ for a set of energies from $\sqrt{s_{NN}} = 10$ GeV up to $\sqrt{s_{NN}} = 200$ GeV. These preliminary results can also be well described within a statistical model of chemical

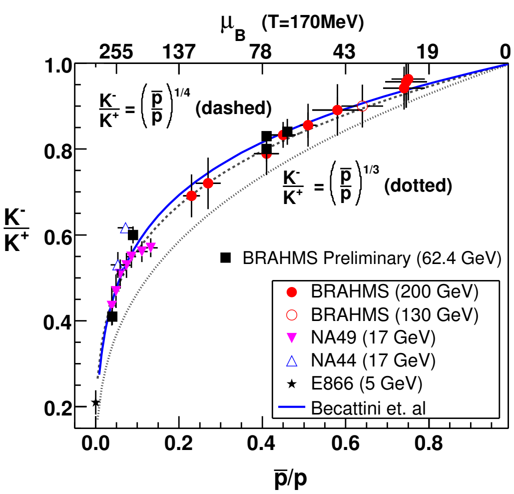

Fig. 1. Correlation between N_{K^-}/N_{K^+} and $N_{\bar{\mathrm{p}}}/N_{\mathrm{p}}$. The solid curve refer to statistical model calculation with a chemical freeze-out temperature of 170 MeV.

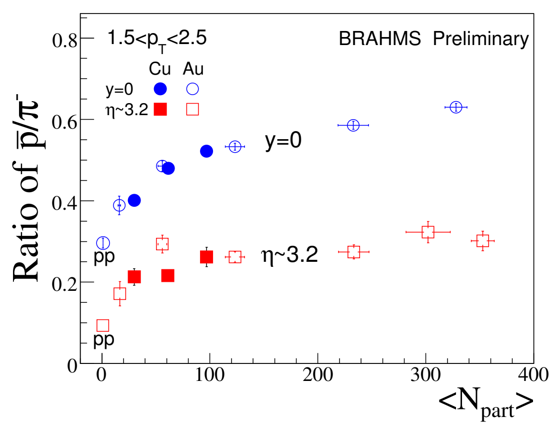

Fig. 2. The averaged $\bar{p}/\pi^-$ versus $\langle N_{part}\rangle$ for Au+Au (open symbols) and Cu+Cu (solid symbols) at $\sqrt{s_{NN}} = 200$ GeV, for $y \approx 0$ (circles) and and for $\eta \approx 3.2$ (squares).

and thermal equilibrium at the quark level and confirm the strong correlation between μ_s and $\mu_{u,d}$ derived from BRAHMS data.

3. Baryon to meson rations

With its excellent particle identification capabilities, BRAHMS can study the p_T and y dependence of hadron production. Preliminary results [17,18] indicate that for Au+Au reactions in the intermediate p_T region the proton to meson ratio is significantly higher than one would expect from the parton fragmentation in vacuum process. Figure 2 shows the $\bar{p}/\pi^-$ centrality dependence for Au+Au (open symbols) and Cu+Cu (solid symbols) at $\sqrt{s_{NN}} = 200$ GeV [19]. The data for $y = 0$ and $\eta \approx 3.2$ are represented by circles and squares, respectively. One can see the strong increase of the $\bar{p}/\pi^-$ ratios as a function of N$_{part}$ in the range $0 < N_{part} < 60$. For $N_{part} > 60$ the dependence starts to saturate and the ratios reach values of about 0.6 and about 0.25 for central collisions at mid- and forward rapidities, respectively. These values exceed the respective values measured in p+p collisions by more than factor 2. For peripheral Au+Au collisions the data approach the p+p results. It is important to note that

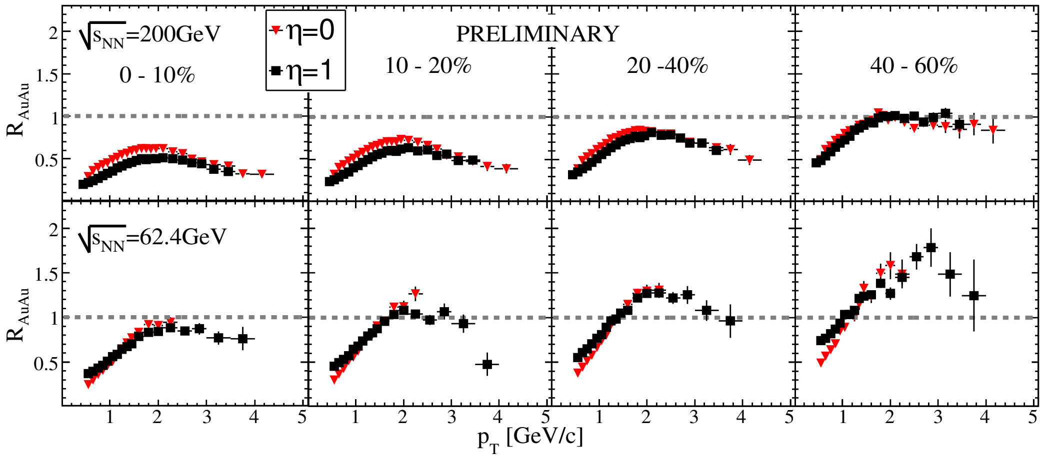

Fig. 3. R_{AA} for charged hadrons measured at $\eta = 0$ and $\eta = 1$ for Au+Au at $\sqrt{s_{NN}} = 200$ GeV (upper row) and at $\sqrt{s_{NN}} = 62.4$ GeV (bottom row), for different centrality bins indicated on the plot (p+p reference for $\sqrt{s_{NN}} = 62.4$ GeV is based on ISR collider data [?]).

the Au+Au and Cu+Cu ratios are consistent with each other when plotted versus $\langle N_{part} \rangle$, indicating that the $\bar{p}/\pi^-$ ratio is controlled by the initial size of the created systems. The observed enhancement in central collisions is consistent with the in-medium parton recombination process which seems to be very efficient mechanism in forming particles at intermediate p_T (2-3GeV/c). The same mechanism would also generate more protons at intermediate p_T, since the momentum of protons would be the sum of momenta of tree partons in constrast to the two required to form a meson [20,21].

4. High p_T suppresion

Particles with high p_T (above 2 GeV/c) are primarily produced in hard scattering processes early in the collision. In high energy nucleon-nucleon reactions hard scattered partons fragment into jets of hadrons. However, in nucleus-nucleus collisions hard scattered partons might travel in the medium. It was predicted that if the medium is a QGP, the partons will loose a large fraction of their energy by induced gluon radiation, effectively suppressing the jet production [22]. Experimentally this phenomenon, known as jet quenching, will be observed as a depletion of the high p_T region in hadron spectra.

We will present results on medium modification through the nuclear modification factor, R_{AA}, defined as the ratio of the particle yield produced in nucleus-nucleus collision, scaled with the number of binary collisions (N_{coll}), and the particle yield produced in elementary nucleon-nucleon collisions:

$$R_{AA} = \frac{Yield(AA)}{N_{coll} \times Yield(NN)}. \qquad (2)$$

4.1. *R_{AA} evolution on collision centrality and collision energy*

Figure 3 shows R_{AA} measured at $\eta = 0$ and $\eta = 1$ for charged hadrons produced in Au+Au reactions at $\sqrt{s_{NN}} = 200$ GeV (upper row) and at $\sqrt{s_{NN}} = 62.4$ GeV (bottom row), for different collision centralities indicated on the plot [23]. For the most central reactions R_{AA} shows suppression for both energies, however, the suppression is significantly stronger at the higher energy. We observe a smooth increase of R_{AA} towards less central collisions, for $\sqrt{s_{NN}} = 200$ GeV, resulting in approximate scaling with N_{coll} for $p_T > 2$ GeV/c for the $40 - 50\%$ centrality bin. However, at $\sqrt{s_{NN}} = 62.4$ GeV, $R_{AA} \approx 1$ for more central collisions, and a Cronin peak is clearly visible already for the $20-40\%$ centrality class, where R_{AA} reaches value of about 1.3 in the p_T range between 2.0 and 3.0 GeV/c. These observations at $\sqrt{s_{NN}} = 62.4$ GeV are qualitatively consistent with a picture in which there are two competing mechanisms that influence the nuclear modification in the intermediate and high p_T range, namely: jet quenching that dominates at central collisions and Cronin type enhancement (k_T broadening or/and quark recombination) that prevails for the more peripheral collisions.

Similar comparison can be done for two different systems, namely Au+Au and Cu+Cu colliding at the same energy ($\sqrt{s_{NN}} = 62.4$ GeV). For Cu+Cu at $\sqrt{s_{NN}} = 62.4$ GeV the same trend of increasing R_{AA} with decreasing collision centrality is seen. However, now the Cronin type enhancement is present already for the most central collisions.

Summarizing the whole set of observations we conclude that the level of suppression of the inclusive hadron spectra produced in nucleus-nucleus collisions at RHIC energies in the p_T range above 2 GeV/c increases with increasing collision energy, collision centrality and with the size of the colliding nuclei. The dependency on the last two variables can be replaced by only one dependency on N_{part} [23].

4.2. *R_{AA} for identified hadrons at forward rapidity for Au+Au at $\sqrt{s_{NN}} = 200$ GeV*

Figure 4 shows the nuclear modification factors found for $(\pi^+ + \pi^-)/2$ (left panel) and $(p + \bar{p})/2$ (right panel), respectively, at $y \approx 3.2$, for central Au+Au reaction [?]. For the comparison we also show the R_{AA} values measured by the PHENIX Collaboration at mid-rapidity. The R_{AA} measured for pions shows strong suppression (by factor of about 3 for $2 < p_T < 3$ GeV/c), both at mid- and at forward rapidity. The consistency between mid- and forward rapidity is seen also for protons, but in this case, R_{AA} reveals a Cronin peak around $p_T = 2$ GeV/c. The similarity between R_{AA} at mid- and forward rapidity observed simultaneously for pions and protons suggests that the same mechanisms are responsible for the nuclear modifications within the studied rapidity interval. Recently, these data have been used to obtain information about the spacial configuration of the deconfined medium by applying perturbative QCD and GLV models [25]. In the proposed picture, at $y \approx 3$, the shorter length of the medium traversed by hardly scattered partons is compensated by larger shadowing effects thus leading to weak dependency of R_{AA} on rapidity as observed experimentally.

5. Summary

The results from BRAHMS and the other RHIC experiments clearly show that studies of high energy nucleus-nucleus collisions have moved to a qualitatively new physics domain. The collisions are characterized by a high degree of reaction transparency leading to the formation of a near-baryon-free central region. From the measurement of charged particle multiplicities in this region lower limits for the energy density at $\tau_o = 1$ fm/c have been determined as 5 GeV/fm^3 and 3.7 GeV/fm^3, for central Au+Au reactions at $\sqrt{s_{NN}} = 200$ GeV and $\sqrt{s_{NN}} = 62.4$ GeV, respectively. Therefore the conditions necessary for the formation of a deconfined system appear to be well fulfilled at RHIC energies. Analysis within the statistical model of the relative abundances of K^-, K^+, p and $\bar{p}$ suggests equilibrium at a chemical freeze-out temperature of 170 MeV, with a noticeably strong correlation between the strange quark and baryon chemical potentials. The p/π ra-

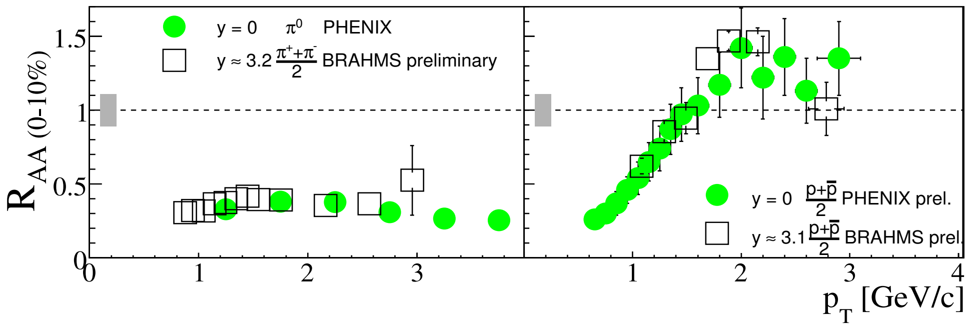

Fig. 4. Comparison of R_{AA} measured for central Au+Au collisions at $\sqrt{s_{NN}} = 200$ GeV, at mid-rapidity and $y \approx 3$ for pions (left panel) and protons (right panel).

tios were measured within $0 < \eta < 3$ for Au+Au and Cu+Cu at $\sqrt{s_{NN}} = 200$ GeV and $\sqrt{s_{NN}} = 62.4$ GeV. The data reveal strong enhancement of baryon to meson ratios in nucleus-nucleus collisions as compared to p+p collisions. Models that incorporate an interplay between soft and hard processes can describe the data at mid-rapidity. We compared R_{AA} for Au+Au at $\sqrt{s_{NN}} = 200$ GeV and $\sqrt{s_{NN}} = 62.4$ GeV, and for Au+Au and Cu+Cu at $\sqrt{s_{NN}} = 200$ GeV. The general observed trend is that R_{AA} increases with: decreasing collision energy, decreasing system size, and when going towards the more peripheral collisions. For Au+Au central collisions at $\sqrt{s_{NN}} = 200$ GeV, R_{AA} shows very weak dependence on rapidity (in $0 < y < 3.2$ interval), both for pions and protons.

References

1. E. V. Shuryak, Phys. Lett. B 78 (1978) 150.
2. J. C. Collins and P. J. Perry, Phys. Rev. Lett. 34 (1975) 1353.
3. BRAHMS experimental home pages: http://www4.rcf.bnl.gov/brahms/WWW/
4. PHENIX experimental home pages: http://www.phenix.bnl.gov/
5. PHOBOS experimental home pages: http://www.phobos.bnl.gov/
6. STAR experimental home pages: http://www.star.bnl.gov/
7. M. Adamczyk *et al.* [BRAHMS Collaboration], Nucl. Instr. and Meth. A 499 (2003) 437.
8. D. Kharzeev and E. Levin, Phys. Lett. B 599 (2001) 79.
9. I. G. Bearden *et al.* [BRAHMS Collaboration], Phys. Lett. B 523 (2001) 227.
10. I. G. Bearden *et al.* [BRAHMS Collaboration], Phys. Rev. Lett. 88 (2002) 202301.
11. G. J. Alner *et al.*, Z. Phys. C 33 (1986) 1.
12. J. D. Bjorken, Phys. Rev. D 27 (1983) 140.
13. I. G. Bearden *et al.* [BRAHMS Collaboration], Phys. Rev. Lett. 94 (2005) 162301.
14. F. Karsch, Nucl. Phys. A 698 (2002) 199.
15. I. G. Bearden *et al.* [BRAHMS Collaboration], Phys. Rev. Lett. 90 (2003) 102301.
16. F. Becattini *et al.*, Phys. Rev. C 64 (2001) 024901.
17. C. E. Jørgensen *et al.* [BRAHMS Collaboration], Nucl. Phys. A 715 (2003) 741c.
18. Z. Yin *et al.* [BRAHMS Collaboration], J. Phys. G 30 (2004) S983.
19. E. J. Kim [BRAHMS Collaboration], Nucl. Phys. A 774 (2006) 493.
20. V. Greco, C. M. Ko, and I. Vitev, *et al.* Phys. Rev. C 71 (2005) 041901R.
21. R. C. Hwa and C. B. Yang, Phys. Rev. C 70 (2004) 024905.
22. X. N. Wang, Phys. Rev. C 58 (1998) 2321.
23. T. M. Larsen [BRAHMS Collaboration], Nucl. Phys. A 774 (2006) 541.
24. R. Karabowicz [BRAHMS Collaboration], Nucl. Phys. A 774 (2006) 477.
25. G. G. Barnaföldi, P. Lévai, G. Papp, and G. Fai, hep-ph/0609023, and references therein.